# Influence of the alloying element Re on the ideal tensile and shear strength of γ′-Ni₃Al

Yun-Jiang Wang[a,*] and Chong-Yu Wang[a,b]

[a]*Department of Physics, Tsinghua University, Beijing 100084, China*
[b]*The International Center for Materials Physics, Chinese Academy of Sciences, Shenyang 110016, China*

The effects of the alloying element Re on the ideal strength of γ′-Ni₃Al under tensile and shear stresses are investigated using the first-principles method. Results for the stress–strain relationships, ideal tensile and shear strenghes with and without Re addition are presented and explained. Re is found to be effective in improving the strength of Ni₃Al. The electronic mechanism underlying the strengthening effects of Re is also elucidated.
© 2009 Acta Materialia Inc. Published by Elsevier Ltd. All rights reserved.

Ni-base single-crystal (SC) superalloys are a very important type of material due to their superior elevated-temperature mechanical properties [1,2]. They are usually used in turbine blades for power generation and advanced aircraft engines. These superalloys are constituted by precipitate γ′ phase (L1₂, ordered face-centered cubic (fcc), Ni₃Al based) and matrix γ phase (disordered fcc, solid solution based on Ni and with a random distribution of different alloying atoms). In general, it is the γ′ phase which is largely responsible for the strength of the superalloys and their resistance to deformation. Therefore, a study of the mechanical behaviors of the γ′ phase should partially reflect the global properties of Ni-base superalloys. Modern commercial superalloys usually contain up to a dozen alloying additions. The strengthening elements in first-generation superalloys include Co, Cr, Ta, Mo, W, etc. However, further improvement in the overall performance of Ni-base SC superalloys requires more refractory elements, such as Re and Ru. The second- and third-generation superalloys contain about 3 and 6 wt.% Re, respectively. Re has been proven to be a critical element for the remarkable improvement of mechanical properties of superalloys [3–5]. However, the strengthening mechanism due to the addition of Re in SC superalloys is not completely understood. According to our knowledge, a first-princi-

ples approach has been extensively adopted to investigate the strengthening mechanism of Re doped in both γ′ phase and γ/γ′ interface systems [6–12]. However, these studies generally focus either on the site preference of alloying elements in γ′ phase or on an energetics analysis combined with electronic structures. Mechanical properties were not emphasized. In particular, no experimental or theoretical study has focused on the effect of Re on the tensile and shear strength of Ni-base superalloys.

The ideal strength of a material, i.e. the stress required to yield or break a perfect crystal, is of great interest in material science. Although the strength of a real crystal can be affected by dislocations, grain boundaries, cracks and other microstructural defects, the ideal strength provides an upper limit of stress before the material fails. Therefore, the study of the ideal strength of a defect-free crystal can provide crucial information to understanding the mechanical properties. Recently, first-principles methods were successfully used to calculate the theoretical strength of materials due to the rapid development of supercomputers [13,14]. The ideal strengths of many metals and intermetallic compounds have been studied and summarized in a review paper of Šob et al. [15]. Ref. [15] also reported the ideal tensile strength of Ni₃Al along the [0 0 1] and [1 1 1] directions. In addition, the effects of boron and sulfur impurities on the ideal tensile strength of Ni₃Al along the [0 0 1] direction were also investigated [16].

* Corresponding author. Tel.: +86 10 62781141; e-mail: wangyunjiang05 @mails.tsinghua.edu.cn

In this paper, we perform first-principles calculations to explore the effects of Re on the ideal strength of $\gamma'$-Ni$_3$Al. The ideal strengths of pure Ni$_3$Al and Ni$_3$Al doped with Re are determined according to the stress–strain relationships. The tensile directions along the [001], [110], [111] and slip systems {111}⟨110⟩, {111}⟨112⟩ are all included in our study. Re is found to improve the ideal strengths considerably. The bonding nature of Re with host atoms is analyzed in terms of charge difference, which provides a deeper insight into the strengthening mechanism of Re in Ni$_3$Al.

The first-principles calculations presented here are based on electronic density-functional theory (DFT), and have been carried out using the VASP code [17]. The generalized gradient approximation (GGA) of projector augmented wave (PAW) [18] is adopted for parametrization of the exchange-correlation function. The cutoff energy of atomic wave functions is set to be 350 eV. The set of $k$ points is chosen according to the size of the supercell with a regular Monkhorst–Pack scheme. In detail, $k$ points of $11 \times 11 \times 15$, and $11 \times 11 \times 8$ are adopted for the tensile [001] (and [110]) direction with and without Re addition. A $5 \times 5 \times 5$ mesh is used for the tensile test along the [111] direction and shear processes. To determine the tensile and shear strength, we adopt the standard approach described in Refs. [13,14]. The stress–strain curves are simulated by incrementally deforming the unit cell in the imposed strain direction. The atomic basis vectors perpendicular to the applied strain are simultaneously relaxed until the other stress components vanish. Meanwhile, all the internal freedoms of the atom are relaxed at each step. The relaxation is done until the forces on all the atoms are less than 0.01 eV/Å. The starting atomic positions at each step are taken from the previous step, which ensures the stress–strain curves are continuous. As described in Refs. [13,14], the uniaxial tensile stress $\sigma$ is derived from $\sigma = \frac{1}{V(\varepsilon)} \frac{\partial E}{\partial \varepsilon}$ and the shear stress $\tau$ from $\tau = \frac{1}{V(\gamma)} \frac{\partial E}{\partial \gamma}$, where

$E$ is the total energy and $V(\varepsilon)$, $V(\gamma)$ are the volumes at the corresponding tensile strain $\varepsilon$ and shear strain $\gamma$.

Figure 1a–c shows the models employed in our calculations. Figure 1b and c are both the refined supercells with specific crystal directions derived from Figure 1a, which is a supercell of $2 \times 2 \times 2$ L1$_2$ Ni$_3$Al unit cells. Figure 1b shows the supercell used to simulate the tensile stress–strain relationships along the [001] and [110] directions. The lower model is twice the size of the upper one along the [001] direction due to the requirement for small Re concentration in $\gamma'$. In fact, the concentration of Re in the present supercell is still much more than that in the experimental alloys. This is because the purpose of the present work is to study the strengthening effect of Re in a qualitative manner. Figure 1c shows the supercells with crystal directions [111], [$\bar{1}$10] and [11$\bar{2}$]. These are used to determine the tensile strength along the [111] direction and shear strengths of the {111}[$\bar{1}$10], {111}[11$\bar{2}$] slip systems. The substitution of Re occupies Al site in Ni$_3$Al according to the results of previous first-principles and experimental site-preference studies [7,9,19].

In order to determine the ideal tensile strength of Ni$_3$Al and Ni$_3$Al doped with Re, two supercells with different symmetries are employed, as shown in Figure 1b and c. The tensile strain directions include [001], [110] and [111]. The tensile strain energies and stresses as a function of strain are shown in Figure 2a and c. We can see from Figure 2a that the strain energy curves are continuous, which indicates the strain path is continuous and confirms the reliability of the method. With the increment of strain, the strain energy along any tensile direction increases until an inflection exists at a finite stain. The inflection corresponds to the maximum stress, which is the ideal tensile strength. In addition, the calculated stress–strain relationships shown in Figure 2c are also continuous.

For the tensile strain of pure Ni$_3$Al along the [001] direction, the stress increases until it reaches a maximum of 26.0 GPa at the strain of 0.32, and then decreases. When doped with Re, the strength remains nearly unchanged with a value of 26.3 GPa. It is also interesting to notice that Ni$_3$Al doped with Re yields at a smaller strain of 0.24. The variation probably has something to do with the bonding nature of Re in the metallic compound, which will be discussed in the following in terms of the charge difference of the Ni$_3$(Al, Re) system.
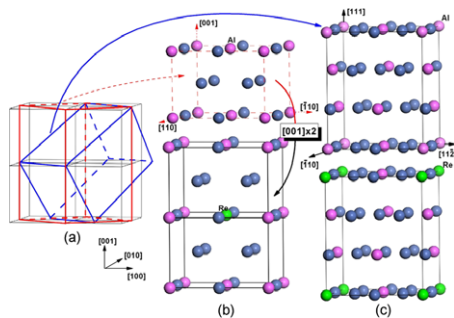


Fig. 1. Configurations of supercells used for the study of tensile and shear strength. The blue, pink and green balls represent Ni, Al and Re atoms, respectively. (a) The black line configuration represents a $2 \times 2 \times 2$ unit cell supercell of Ni$_3$Al, in which the red and blue configurations are the supercells with specific crystal directions. (b) The upper cell is used for the tensile test in the [001] and [110] directions, while the lower cell is two times of upper one in the [001] direction doped with Re. (c) The upper structure is the supercell used for the Ni$_3$Al tensile test in the [111] direction and shear test in the {111}[$\bar{1}$10], {111}[11$\bar{2}$] slip systems, the lower structure is the corresponding supercell doped with Re. (For interpretation of the references to colour in this figure legend, the reader is referred to the web version of this article.)
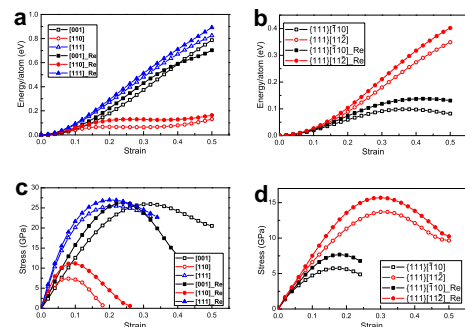


Fig. 2. Energy-strain per atom and stress–strain relationships: (a and c) under tension; (b and d) under shear.

In contrast with the [0 0 1] loading direction, the substitution of Re considerably improves the ideal tensile strength along both the [1 1 0] and [1 1 1] directions. Without Re addition, the ideal strengths for these two directions are 7.4 and 25.4 GPa, respectively. The addition of Re increases the values to 11.2 and 27.0 GPa, respectively. The results show that Re is effective in improving the ideal tensile strength of $Ni_3Al$ along the [1 1 0] and [1 1 1] tensile directions. However, the strengthening effect along the [0 0 1] direction is not obvious. Moreover, it should be pointed out that the concentration of Re addition in the [0 0 1] (and [1 1 0]) tensile directions is different from that of the [1 1 1] tensile direction shown in Figure 2a and c. To test the effect of Re concentration on the strength, we also simulate the [1 1 0] tensile process with the supercell shown in Figure 14b, upper. In contrast with the 16 atom model, this yields a higher tensile strength of 13.7 GPa along the [1 1 0] direction. The result is reasonable because the greater the Re addition in $Ni_3Al$, the more Re–Ni covalent-like bonds exist.

In addition to the tensile process and the ideal tensile strength of $Ni_3Al$ with and without Re, the shear process and shear strength are also considered in our study. The shear strength of a material is difficult to measure experimentally. Therefore, a theoretical investigation into the effect of Re on the shear behaviors of $Ni_3Al$ based on DFT is necessary. We have performed first-principles ideal shear test for two typical slip systems $\{1 1 1\}[\bar{1} 1 0]$ and $\{1 1 1\}[1 1 \bar{2}]$ in our calculations.

The energy–strain and stress–strain relationships for shear process of $Ni_3Al$ with and without Re impurity are shown in Figure 2b and d, respectively. For the $\{1 1 1\}[\bar{1} 1 0]$ shear direction, the strain energy of $Ni_3Al$ increases as the strain increases, then an inflection point occurs at a strain of 0.18. Correspondingly, the stress reaches its maximum of 5.8 GPa at $\gamma = 0.18$. Thus, the ideal shear strength for the $\{1 1 1\}[\bar{1} 1 0]$ direction is 5.8 GPa. When doped with Re, the strain energy increases compared to pure $Ni_3Al$. As a result, the maximum stress is correspondingly raised to 7.7 GPa, an increment of 33%. The effect of Re on the $\{1 1 1\}[1 1 \bar{2}]$ shear process of $Ni_3Al$ is similar. The addition improves the ideal strength from 13.7 to 15.7 GPa, which can be seen in Figure 2d.

For comparison, we have listed all the ideal tensile and shear strengths of $Ni_3Al$ with and without Re in Table 1. We can see that the effect of Re on the strength of $Ni_3Al$ is obvious. Except for tensile strength along the [0 0 1] direction, all the ideal strengths considered in our study are improved considerably by Re. The reason is that the distance between Re and host atoms along the
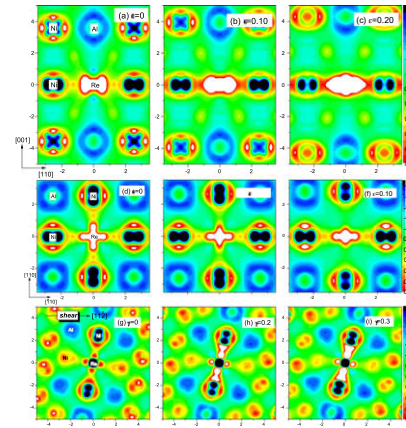


**Fig. 3.** (a–c) The charge density difference on the (1 0 0) planes of $Ni_3(Al, Re)$ at different tensile strains during the [0 0 1] loading process; and (d–f) on the (0 0 1) planes at different tensile strains. (g–i) on a crystal plane containing Re addition during the shear process in the $\{1 1 1\}[1 1 \bar{2}]$ slip system. Positive (negative) values denote charge accumulation (depletion).

[0 0 1] direction is too long, and their interactions are too weak to influence the tensile strength.

In order to gain a deeper insight into the origin of the strengthening effect of Re, we have also calculated the charge density difference of $Ni_3Al$ doped with Re at different strains. The charge density difference of the $Ni_3(Al, Re)$ system is defined as $\Delta\rho = \rho[Ni_3(Al, Re)] - \rho_{free}[Ni_3(Al, Re)]$, where $\rho_{free}$ is the superposition of the free atom charge density. The charge redistribution induced by impurities can directly reflect the bonding nature of atoms. The bonding characteristics between impurity Re and host atoms may correlate strongly with the improvement of mechanical properties of $Ni_3Al$. Figure 3 shows the charge difference of $Ni_3(Al, Re)$ systems at different tensile and shear strains. The charge difference on the (1 1 0) planes during the process of [0 0 1] loading at strains $\varepsilon = 0$, 0.10, 0.20 is plotted in Figure 3a–c, respectively. Figure 3d–f is the charge differences on the (0 0 1) planes during the process of [1 1 0] loading, with tensile strains of $\varepsilon = 0$, 0.04, 0.10, respectively.

From the [0 0 1] loading process shown in Figure 3a–e, it is clear to see that the strong charge accumulation regions appear between Re and its nearest neighbor (NN) Ni atoms along the [1 1 0] direction. In contrast, almost no charge redistribution exists along the [0 0 1] direction. These kinds of charge redistributions lead to strong directional bonding in the [1 1 0] direction, whereas the bonding in the [0 0 1] direction is much weaker. As the strain increases, the distance between atoms along the [0 0 1] direction becomes longer, whereas the distance between Re and its NNs along the [1 1 0] direction becomes shorter. The applied tensile strain results in the bonding along the [0 0 1] directions becoming weaker, while the bonding along the [1 1 0] directions becomes stronger. This is the reason why the addition of Re has almost no effect on the ideal tensile strength of $Ni_3Al$ along the [0 0 1] direction. Furthermore, the directional bonding between Re and Ni is covalent-like. It is more brittle than the metallic bonding between the host atoms

**Table 1.** Calculated ideal tensile strength $\sigma$ and shear strength $\tau$ (GPa) with the corresponding strain at which the maximum stress occurs.

| Direction | $Ni_3Al$ | | $Ni_3Al$ with Re | |
|---|---|---|---|---|
| | $\sigma$ | $\varepsilon$ | $\tau$ | $\gamma$ |
| [0 0 1] | 26.0 | 0.32 | 26.3 | 0.24 |
| [1 1 0] | 7.4 | 0.08 | 11.2 | 0.10 |
| [1 1 1] | 25.4 | 0.22 | 27.0 | 0.20 |
| $\{1 1 1\}[\bar{1} 1 0]$ | 5.8 | 0.18 | 7.7 | 0.18 |
| $\{1 1 1\}[1 1 \bar{2}]$ | 13.7 | 0.32 | 15.7 | 0.30 |

themselves. This bonding nature may correlate with the result that doped Ni$_3$Al yields at a smaller strain.

During the tensile process along the [1 1 0] direction, the charge redistribution changes more obviously than [0 0 1] loading. Charge difference regions clearly appear around Re in the equilibrium structure shown in Figure 3d. Therefore, the bonding between Re and its NN Ni atoms is strongly directional along the [1 1 0] crystal direction. The covalent bond characteristic is very clear. The covalent-like bond along the [1 1 0] direction will resist the tensile deformation, leading to higher strength. The result is consistent with the finding that Re considerably improves the tensile strength along the [1 1 0] direction. Moreover, the charge accumulation along the [1 1 0] direction is becoming increasingly weaker during the tensile process. In particular, it can be noted from Figure 3f that the Re–Ni bond along the tensile direction breaks at the strain $\varepsilon = 0.10$. The strain $\varepsilon = 0.10$ corresponds to the yield point of the [1 1 0] tensile direction, which can be seen in Figure 2c.

Similarly to tensile strains, Figure 3g–i shows the charge difference on a crystal plane including both Re and its neighbor host atoms during the process of shear deformation along the $\{1 1 1\}[1 1\bar{2}]$ direction. It can be seen that strong directional bonds exist between Re and NN Ni atoms due to charge difference at equilibrium (Fig. 3g). Following the evolution of the charge difference, we find that the Re–Ni bond nearly along the $[1 1\bar{2}]$ direction starts to weaken. On the other hand, the Re–Ni bond nearly perpendicular to the $[1 1\bar{2}]$ direction becomes stronger as the shear strain evolves. The strong directional Re–Ni bonds effectively resist the shear deformation, and result in a higher shear strength of Ni$_3$Al. This is the electronic mechanism underlying the strengthening effect of Re on the mechanical properties of $\gamma'$-Ni$_3$Al.

The first-principles method has been employed to study the effect of alloying element Re on the ideal tensile and shear strengths of $\gamma'$-Ni$_3$Al. The calculated results for stress–strain relationships, ideal tensile and shear strengths of pure Ni$_3$Al and of the Re-doped Ni$_3$(Al, Re) system have been presented. Our results show that the addition of Re considerably improves both the tensile and shear strength of Ni$_3$Al. A detailed analysis of the charge difference of the Ni$_3$(Al, Re) system during the process of both tensile and shear deformation is also provided. Results show that the

covalent-like Re–Ni bond effectively resists the deformation of Ni$_3$Al, and leads to a higher strength. This is the electronic mechanism underlying the strengthening effects of Re.

[1] C.T. Sims, Superalloy II, John Wiley, New York, 1987, pp. 97–131.
[2] Q. Feng, T.K. Nandy, S. Tin, T.M. Pollock, Acta Mater. 51 (2003) 269.
[3] A. Giamei, D.L. Anton, Met. Trans. A 16A (1997) 1985.
[4] A.D. Cetel, D.N. Duhl, in: Second Generation Columnar Grain Nickel-Base Superalloy, The Minerals, Metals & Materials Society, Warrendale, PA, 1992, pp. 287–296.
[5] B.D. Bryskin (Ed.), Rhenium and Rhenium Alloys, The Minerals, Metals & Materials Society, Warrendale, PA, 1997, pp. 731–754.
[6] C.Y. Geng, C.Y. Wang, et al., Acta Mater. 52 (2004) 5427.
[7] S.Y. Wang, C.Y. Wang, et al., Phys. Rev. B 65 (2001) 035101.
[8] P. Peng et al., Comp. Mater. Sci. 38 (2006) 354.
[9] K. Chen, L.R. Zhao, J.S. Tse, Acta Mater. 51 (2003) 1079.
[10] K. Chen, L.R. Zhao, J.S. Tse, Philos. Mag. 83 (2003) 1685.
[11] Y.J. Wang, C.Y. Wang, Mater. Sci. Eng. A 490 (1999) 242.
[12] Y.J. Wang, C.Y. Wang, J. Appl. Phys. 104 (2008) 013109.
[13] D. Roundy, C.R. Krenn, M.L. Cohen, J.W. Morris, Phys. Rev. Lett. 82 (1999) 2713.
[14] D. Roundy, C.R. Krenn, M.L. Cohen, J.W. Morris, Philos. Mag. A 81 (2001) 1725.
[15] M. Šob, M. Friák, D. Legut, J. Fiala, V. Vitek, Mater. Sci. Eng. A 387–389 (2004) 148.
[16] S.N. Sun, N. Kioussis, M. Ciftan, Phys. Rev. B 54 (1996) 3074.
[17] G. Kresse, J. Hafner, Phys. Rev. B 48 (1993) 13115.
[18] G. Kresse, J. Joubert, Phys. Rev. B 59 (1999) 1758.
[19] Y. Zhou, Z.G. Mao, C. Booth-Morrison, D.N. Seidman, Appl. Phys. Lett. 93 (2008) 171905.